

# Digital image processing techniques for the analysis of fuel sprays global pattern

Rami Zakaria<sup>1</sup>, Peter Bryanston-Cross<sup>2</sup> and Brenda Timmerman<sup>2</sup>

<sup>1</sup>Department of Mechanical System Engineering, Hansung University, Seoul, S. Korea

<sup>2</sup>School of Engineering, Warwick University, Coventry, UK

\*E-mail: dr.rami.zakaria@gmail.com

**Abstract.** We studied the fuel atomization process of two fuel injectors to be fitted in a new small rotary engine design. The aim was to improve the efficiency of the engine by optimizing the fuel injection system. Fuel sprays were visualised by an optical diagnostic system. Images of fuel sprays were produced under various testing conditions, by changing the line pressure, nozzle size, injection frequency, etc. The atomisers were a high-frequency microfluidic dispensing system and a standard low flow-rate fuel injector. A series of image processing procedures were developed in order to acquire information from the laser-scattering images. This paper presents the macroscopic characterisation of Jet fuel (JP8) sprays. We observed the droplet density distribution, tip velocity, and spray-cone angle against line-pressure and nozzle-size. The analysis was performed for low line-pressure (up to 10 bar) and short injection period (1-2 ms). Local velocity components were measured by applying particle image velocimetry (PIV) on double-exposure images. The discharge velocity was lower in the micro dispensing nozzle sprays and the tip penetration slowed down at higher rates compared to the gasoline injector. The PIV test confirmed that the gasoline injector produced sprays with higher velocity elements at the centre and the tip regions.

## 1. Introduction

The function of a fuel injector is to deliver individual pulses of fuel into the combustion chamber of an internal combustion engine. Liquid fuels are turned into sprays by increasing the relative velocity between the fluidic phase and the surrounding ambient. This technique is referred to as ‘fluid atomisation’. In pressure-based injectors, the fuel is pressurised into a narrow orifice. The average droplet size of the resultant spray is directly related to the design and quality of that atomiser and on the applied pressure; the more effective a fuel atomiser, the smaller droplets it produces. By reducing the mean droplet diameter, the overall surface area of the fuel increases, which improves the evaporation rate and the burning range. This leads to higher rates of released power during the combustion process and lower exhausted pollutant emissions. Beside the droplet size, other global parameters are of importance to engine manufacturers, such as the spray development velocity and the spray pattern. Understanding the behaviour of fluid sprays, therefore, is vital for designing fuel injectors [1-4].

Spray formation process is a complex problem with many parameters involved, such as nozzle geometry and design [5-10], pressure [4,11,12], cavitation [13,14], evaporation [15], viscosity [16-18], surface tension [18], and temperature [19]. Optical techniques provide invaluable information about



spray characteristics. Among all optical methods, imaging methods are dominant in the area of experimental characterization thanks to the advances in digital imaging. Modern digital cameras produce high resolution images that can be enhanced and processed in order to characterise the fluid sprays. The focus of most researchers is on diesel and gasoline direct injection techniques under very high-pressure levels (higher than 100 bar). This paper presents visualisation and processing techniques for the analysis of a kerosene-based (aviation) fuel. It discusses the spray global characteristics and development process against line-pressure and time after-start-of-injection (ASOI).

Small rotary engines are useful in various high power-to-weight applications today, such as racing vehicles, robots, and unmanned aerial vehicles (UAVs). In this type of engine, understanding the spray development process can help in optimizing the combustion process. This becomes especially necessary when the time available for atomisation, vaporization and mixing with air is relatively short. We studied the manifold (indirect) injection strategy in a high-speed (15,000 -18,000 rpm) rotary (Wankel) engine. Due to the small manifold size and the high injection rate, timing the injection pulse (against rotor angle and ignition spark) was crucial. The engine was required to operate on (JP8) jet-fuel and line low-pressure (less than 10 bar). Very little work has been reported on both low-pressure injection and kerosene-like fuels in literature.

We developed a visualisation system and an image processing procedure for spray characterization. Our experiments on heavy jet fuel injectors yielded to around 2.4 Tb of data in form of digital images. Therefore, the image processing techniques needed to be planned carefully to present the outcomes of our analysis in an efficient manner.

## 2. Experimental conditions

Aviation (JP8) fuel sprays were produced by two injectors using a maximum line-pressure of 10 bar into an unpressurised ambient. The first injector was a standard 12 V electric gasoline injector (single hole,  $D_o=584 \mu\text{m}$ ,  $f_{\text{max}}=0.4 \text{ kHz}$ ,  $P_{\text{max}}=5 \text{ bar}$ ). The second injector was a high-frequency micro dispensing nozzle (single hole,  $D_o=255 \mu\text{m}$ ,  $f_{\text{max}}=2.2 \text{ kHz}$ ,  $P_{\text{max}}=10 \text{ bar}$ ), which was originally developed for medical purposes and never used for fuel injection before. JP8 is commonly used in turbine-engine aircrafts. We have found that a JP8 fuel drop  $35 \mu\text{m}$  in diameter needs approximately 1.2 ms to start evaporating at  $500 \text{ }^\circ\text{C}$  in atmospheric pressure. The temperature of the manifold (in our case and in most of the similar rotary engines) does not exceed  $50 \text{ }^\circ\text{C}$  when the engine is hot, and it is much lower in the cold-start case. Therefore, it is safe to assume that all the evaporation happens inside the combustion place rather than in the manifold. In rotary engines, the fuel mixture is “sucked into” the combustion place by the pressure difference created by the rotor motion. The mixture is then pressurized and ignited, typically by multiple spark plugs. It is important that the fuel is well mixed with air before the suction stage. This study investigates the fuel spray development process inside the injection manifold, just before introducing the fuel mixture into the combustion place. A sufficient penetration of the liquid fuel within the injection manifold can improve the fuel-air mixing. But if a spray ‘grows’ faster than the fuel intake rate, this may increase the wall wetting, and hence, the unburned hydrocarbons. Therefore, understanding the spray development process is useful for engine design, and also for the development of computational models for engine performance optimization [4]. The engine was a single rotor Wankel engine, which weighed less than 5 kg and produced around 8.5 hp (6.3 kW) of power at 9200 rpm. The small physical dimensions of the engine introduced challenges in terms of producing a fast evaporation rate and atomising using low pressure levels.

Spray images were acquired in a dark isolated cell where all devices were remotely controlled. Strict health and safety regulations were applied due to the explosive nature of the fuel and the risk of direct exposure to class-4 and class-3 laser beams.

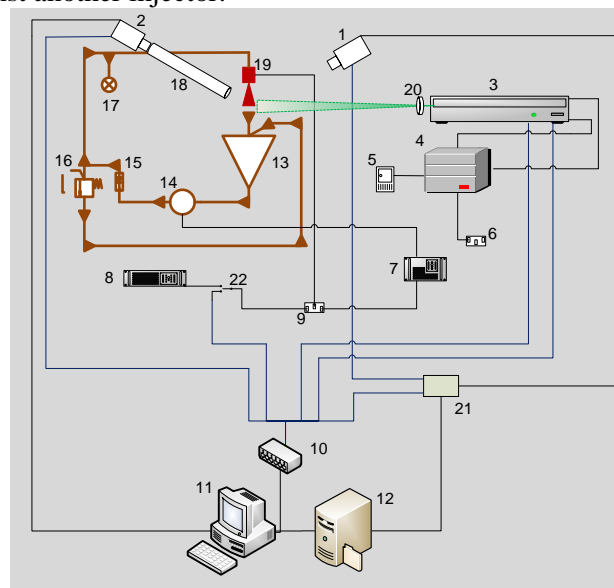
## 3. Visualisation system

Figure 1 shows the developed optical diagnostic system for spray visualisation [20]. The laser beam was generated by a double-pulse Nd:YAG green laser (532 nm wavelength), and then turned into a thin laser sheet (around 3 mm in width at the imaging plane). The maximum optical power of the laser

device was 600 mJ during a pulse-width as short as 4 ns. Two CCD cameras (Table.1) acquired the images at both macroscopic and microscopic levels. A controller synchronised the injection pulses with the laser pulses and the camera exposure using a programmable hardware with a TI-MSP430 microcontroller core and an embedded-C program. A Scheimpflug adaptor was mounted between the lens and the photo-sensor to keep the object plane is in sharp focus.

The cameras produced double-frame images for particle image velocimetry PIV tests. The time interval was 12-50  $\mu\text{s}$  between the frame couples and 25-50  $\mu\text{s}$  between the test points (depending on the spray maximum velocity). The result of each test point was represented by the average of 250-500 images, compared to 5-50 images reported in most similar experiments.

This system was previously employed to calculate the tip penetration velocity and the microscopic velocity using micro-PIV for a standard gasoline injector ( $D_o=584 \mu\text{m}$ ) [20]. In the current paper, the results are compared against another injector.



**Figure 1.** The spray visualisation rig for high-speed spray jet: (1) high resolution first CCD camera, (2) second CCD camera, (3) Nd:YAG laser head, (4) laser power supply, (5) laser controller, (6) 3-Amps AC main power, (7) adjustable DC power supply, (8) TTL signal generator, (9) injector driver circuit, (10) PC-control unit, (11) control PC, (12) data storage RAID, (13) fuel supply, (14) fuel pump, (15) flow control, (16) pressure relief valve, (17) pressure gauge, (18) K2 microscope, (19) fuel Injector, (20) laser sheet optics, (21) PCO camera controller, (22) trigger switch.

**Table 1.** Cameras specifications in the spray visualisation system.

	PCO Pixelfly	PCO 2000
<b>Resolution (pixel)</b>	1360 x 1024	2048 x 2048
<b>Frame-rate (Hz, Max)</b>	50	14.7
<b>Inter-frame time (ns)</b>	5000	180
<b>Dynamic Range (bits)</b>	12	14
<b>Exposure (<math>\mu\text{s}</math>, Min)</b>	5	0.5

#### 4. Results and discussion

The mean-image was calculated at each test point. The mean-images were then binarized by a threshold that separated the spray pixels from the background. Due to the low density of the sprays, it

was necessary to fill up the gaps within the spray image using a filter (3x3 mask) that compares each pixel with its neighboring pixels. Finally an edge detection procedure defined the spray boundaries using a 2D-median filter. Figure 2 shows the steps of acquiring the spray profile of the micro dispensing valve using a series of injection pulses (416.7 Hz, 50% duty-cycle). The resulting images directly provided the cone-angle and the sheet area.

We also analysed spray images at several stages of the injection cycle to observe the fluid disintegration process step by step. Figure 3 shows example images using a standard gasoline injector at 5-bar line-pressure. The injector valve was opened for 1.2 ms and closed for another 1.2 ms. The sequenced images show that the primary atomisation started 300  $\mu$ s ASOI. At 450 ASOI the fluid bulk started disintegrating off the jet surface. The disintegration process continued as the jet penetrated further downstream of the nozzle. By the end of the injection pulse, it could be seen that the small droplets produced by the early atomisation stage stayed behind and moved much slower than the central jet. The breakup of the central jet happened after the end of the injection pulse, producing only large droplets. The average penetration by the end of the injection pulse was approximately 38 mm for the 5 bar line-pressure, compared to 20 mm using 3 bar line-pressure.

In this part of the experiment, the focus was on the central jet progression using a standard (55 mm) lens. Droplets that are less than 50  $\mu$ m in diameter were visible to the microscope only. This is because the diffraction efficiency in the case of large fluid drops is much higher than in the small droplets at the 90° angle of observation [21]. The flow-rate distribution measurements (using mechanical patternators) showed that for the gasoline injector almost 40% of the injected fluid stays at the central part of the spray (less than 20° divergence angle), compared to 28% for the micro dispensing valve. The central part of the spray represents the poorly atomised liquid, while the fine droplets are drifted away towards the peripheries.

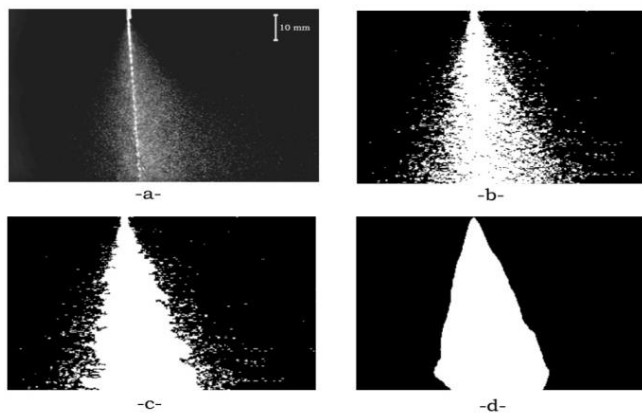


**Figure 2.** Spray boundaries detection by image processing of a micro dispensing valve at 3 bar: (a) mean-image, (b) black and white image, (c) gaps filled up, (d) spray boundaries by edge detection. The angle between the laser sheet and the camera sensor was 60° (focus was corrected by a Scheimpflug adaptor).

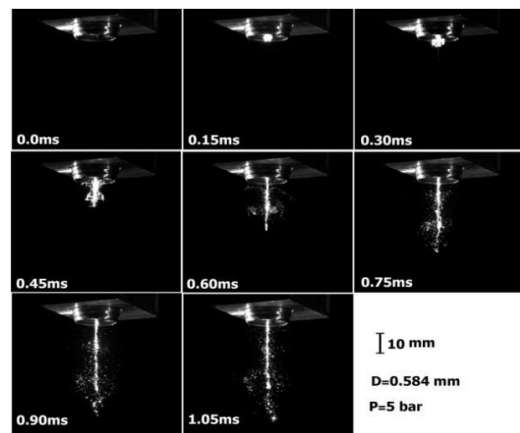


**Figure 3.** Images of the JP8 spray during an injection pulse of 1.2 ms using a gasoline injector ( $D_0=584 \mu\text{m}$ ). Images were taken for several injection incidents using a 2 mm laser sheet (4 ns optical pulse-width). The angle between the laser sheet and the camera sensor was 90°.

The tip penetration measurements (Figure 4) show that sprays penetrated around 7 cm by the end of the injection pulse for both nozzles at  $P_{in}=5$  bar, compared to around 3 cm at  $P_{in}=4$  bar. The discharge velocity was lower in the micro nozzle sprays than in the gasoline injector. The tip velocity of the micro nozzle sprays dropped at higher rates than the gasoline injector sprays, which was an indication for a better atomisation at the centre of the jet. Figure 5 shows the tip velocity calculated from the tip penetration results by calculating the first derivative of the third order polynomial fit of

the graphs in Figure 4. The tip velocity decreased at higher rates for sprays produced by high pressure levels.

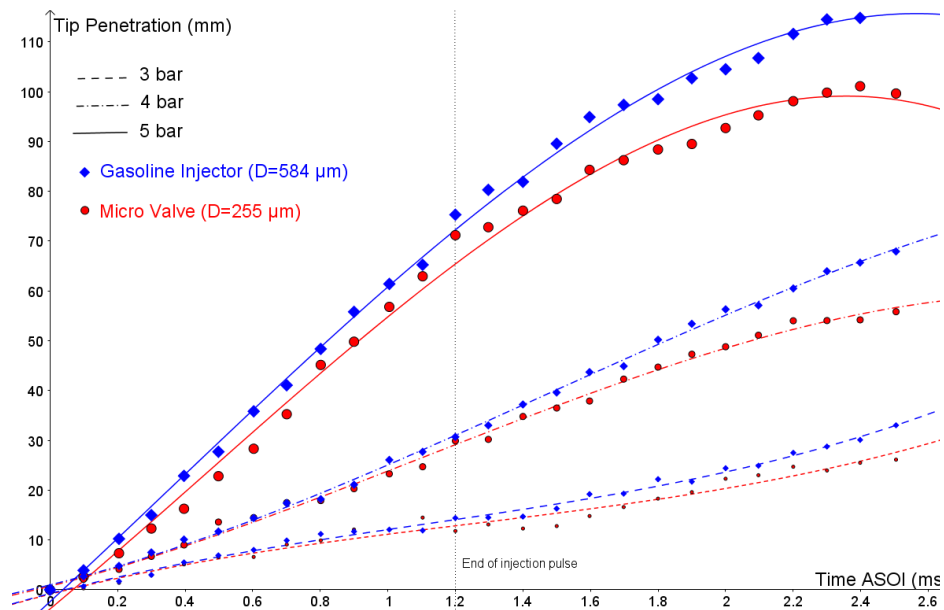


**Figure 4.** Tip penetration for JP8 sprays against time ASOI ( $P_{in} = 3,4,5$  bar) for the two tested nozzles.

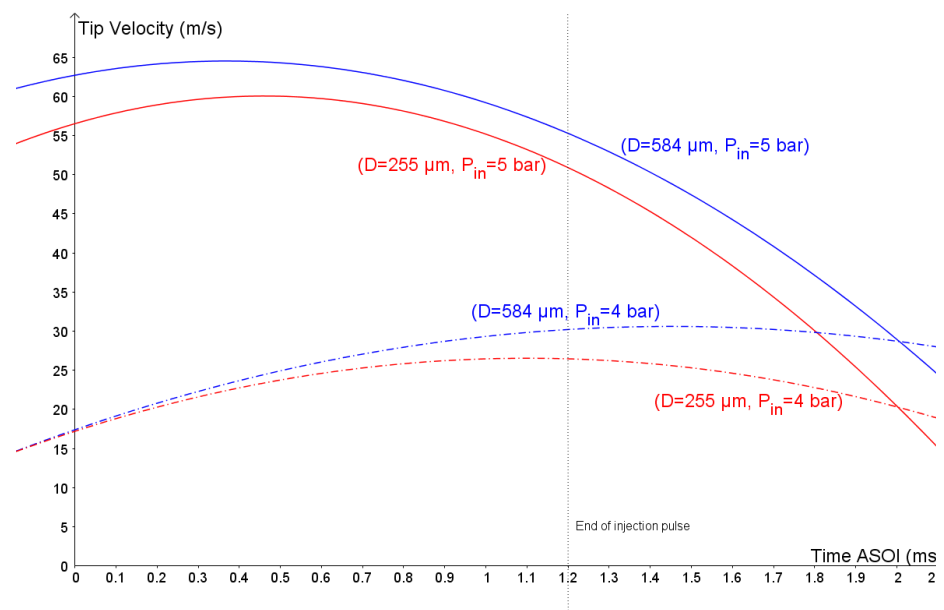


**Figure 5.** Tip velocity for JP8 sprays against time ASOI ( $P_{in} = 4,5$  bar) estimated from the tip penetration data.

The colour coded mean-image of the fully developed spray (Figure 6) provides a statistical prospective of the spray density distribution. The middle highly dense region of the fluid jet penetrated far downstream of the injector's nozzle, while low droplet density with lower velocity elements (due to the smaller mean droplet diameter) scattered to wider angles. Although the gasoline injector had a larger discharge angle closer to the orifice (due to its larger orifice diameter), most of the high density elements were concentrated in the middle of the spray jet. In contrast, the middle of the spray produced by the micro dispensing nozzle disintegrated into smaller elements that diverged into wider

angles further downstream. The density maps provide a good representation of how the fluid volume is distributed throughout the spray area. The local velocity for these elements was measured by a particle image velocimetry (2D-PIV) analysis.

PIV is a well-established non-intrusive measurement technique in fluid mechanics, where the velocity vector field is generated by calculating the displacement of the particles between two successive frames. Each frame is divided into fixed size interrogation windows. Each window from the first frame is compared by the corresponding window from the second frame by calculating the mathematical cross-correlation. The velocity vector field (Figure 7) shows that at the middle jet velocity was 30-35 m/s at the end of the injection pulse. This is comparable to what we have found in the tip velocity graphs (Figure 5), where 30 m/s was estimated for the gasoline injector and 26.6 m/s for the micro dispensing system at the same instant ASOI. It is possible to see a higher concentration of the high velocity elements at the middle and the tip regions in the gasoline injector case. It shows that the micro dispensing nozzle performs earlier atomisation than the gasoline injector, and this is especially useful in the event of engine's cold start.

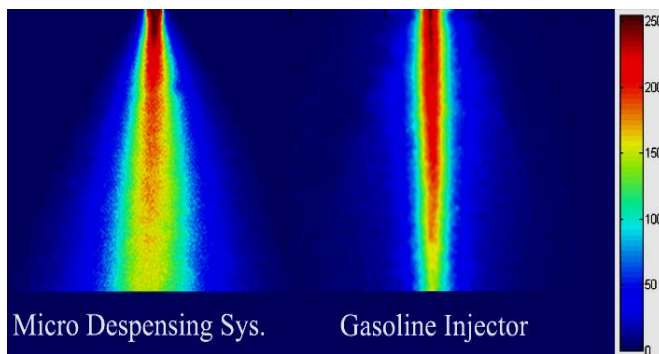


**Figure 6.** The fluid density distribution represented by the average pixel intensity of spray images for a standard gasoline injector and a micro dispensing nozzle ( $P_{in}=4$  bar,  $T=1.2$  ms ASOI, continuous injection).

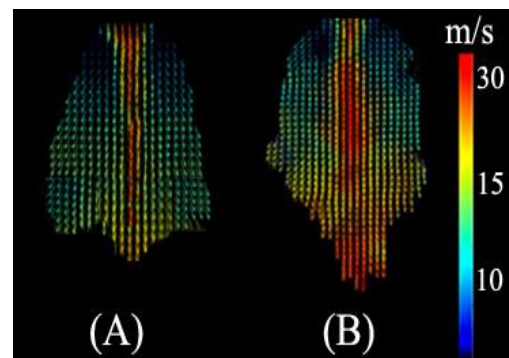


**Figure 7.** Velocity vector fields of JP8 fuel sprays ( $T=1.2$  ms ASOI,  $P_{in}=4$  bar) by two-stage cross-correlation for (A) a micro dispensing nozzle, (B) a gasoline injector.

## 5. Conclusions

We studied JP8 fuel sprays produced by two fluid atomisers. The first atomiser was a standard gasoline injector for low-flow rate applications. The second was a light-weight high-frequency micro-dispensing system. The fuel sprays were visualised using a laser-sheet imaging technique and acquired the macroscopic characteristics of the sprays with image processing. Understanding the development process of fuel sprays is important when designing engines, especially small rotary engines, where time available for atomisation, vaporization and mixing with air is relatively short.

The discharge velocity was lower in the micro dispensing nozzle sprays than in the gasoline injector. However, the tip velocity of the micro nozzle sprays dropped at higher rates for the micro dispensing nozzles and for high pressure rates. The micro dispensing nozzle seemed to perform an earlier atomisation than the gasoline injector, producing low-speed small droplets that scatter at wider angles. The PIV test confirmed that the standard gasoline injector produced sprays with higher velocity at the centre and the tip regions. These results are to be confirmed in the future by droplet size and velocity distribution analysis using long-range microscopy.

## Acknowledgments

The authors would like to thank the Optical Engineering Laboratory (OEL) team at the University of Warwick, and Cubewano Ltd R&D team for their support of the work presented in this paper. This work was financially supported by Hansung University.

## References

- [1] Crua C, Heikal M R and Gold M R 2015 Microscopic imaging of the initial stage of diesel spray formation *Fuel* **157** pp 140-50
- [2] Dong Q, Ishima T, Kawashima H and Long W 2013 A study on the spray characteristics of a piezo pintle-type injector for DI gasoline engines *Journal of Mechanical Science and Technology* **27**(7) pp 1981-93
- [3] Costa M, Sorge M and Allocca L 2012 Increasing energy efficiency of a gasoline direct injection engine through optimal synchronization of single or double injection strategies, *Energy Conversion and Management* **60** pp 77–86
- [4] Hiroyasu H and Arai M 1990 Structures of fuels sprays in Diesel engines *SAE technical paper* 900475
- [5] Payri R, Viera J P, Gopalakrishnan V and Szymkowicz P G 2017 The effect of nozzle geometry over the evaporative spray formation for three different fuels *Fuel* **188** pp 645-60
- [6] Payri R, Viera J P, Gopalakrishnan V and Szymkowicz P G, 2016 The effect of nozzle geometry over internal flow and spray formation for three different fuels *Fuel* **183** pp 20–33
- [7] Lad V N and Murthy Z V P 2016 Effects of the geometric orientations of the nozzle exit on the breakup of free liquid jet *Journal of Mechanical Science and Technology* **30** (4) pp 1625-30
- [8] Yoon S H, Kim D Y, Kim D K and Kim B H 2011 Effect of nozzle geometry for swirl type twin-fluid water mist nozzle on the spray characteristic, *Journal of Mechanical Science and Technology* **25** (7) pp 1761-66
- [9] Liu Z, Im K S, Wang Y, Fezzaa K, Wang J, Xie X B, Lai M C and Wang J 2010 Near-nozzle structure of diesel sprays affected by internal geometry of injector nozzle: visualized by single-shot X-ray imaging *SAE technical paper* 2010-01-0877
- [10] Han J S, Lu P H, Xie X B, Lai M C and Henein N A 2002 Investigation of diesel spray primary break-up and development for different nozzle geometries, *SAE technical paper* 2002-01-27
- [11] Chen P C, Wang W C, Roberts W L and Fang T 2013 Spray and atomization of diesel fuel and its alternatives from a single-hole injector using a common rail fuel injection system *Fuel* **103** pp 850-61
- [12] Delacourt E, Desmet B and Besson B 2005 Characterisation of very high pressure diesel sprays using digital imaging techniques *Fuel* **84** (7) pp 859-67
- [13] Suh H K and Lee C S 2008 Effect of cavitation in nozzle orifice on the diesel fuel atomization characteristics *Int. J. Heat Fluid Flow* **29** (4) pp 1001–09
- [14] Blessing M, König G, Krüger C, Michels U and Schwarz V 2003 Analysis of flow and cavitation phenomena in diesel injection nozzles and its effects on spray and mixture formation *SAE technical paper* 2003-01-1358
- [15] Naber J D and Siebers D L 1996 Effects of Gas Density and Vaporization on Penetration and Dispersion of Diesel Sprays *Transactions of the SAE* 960034
- [16] Harris A S, Svensson E, Wagner Z G, Lethagen S and Nilsson I M 1988 Effect of viscosity on particle size, deposition, and clearance of nasal delivery systems containing desmopressin *Journal of pharmaceutical sciences* **77** (5) pp 405-408
- [17] Arai M, Tabata M, Hiroyasu H and Shimizu M 1984 Disintegrating process and spray characterization of fuel jet injected by a diesel nozzle *SAE Technical Paper* 840275
- [18] Lefebvre A 1988 *Atomization and sprays* (CRC press) vol 1040 no 2756
- [19] Payri R, Garcia-Oliver J M, Bardi M and Manin J 2012 Fuel temperature influence on diesel sprays in inert and reacting conditions *Applied Thermal Engineering* **35** pp 185-95
- [20] Zakaria R, Bryanston-Cross P and Timmerman B 2014 Spray development process of aviation fuel using a low-pressure fuel injector: Visualization and analysis *Journal of Mechanical Science and Technology* **28** (12) pp 5003-11
- [21] Zakaria R and Bryanston-Cross P 2012 Light scattering efficiency of oil smoke seeding droplets in PIV systems *IEEE Photonics Global Conference (PGC)* pp 1-5